

Model independent interpretation of recent CR lepton data after AMS-02

Daniele Gaggero^{a,b} Luca Maccione^{c,d}

^aSISSA, via Bonomea 265, 34136 Trieste (Italy)

^bINFN, Sezione di Trieste, via Valerio 2, 34127 Trieste (Italy)

^cArnold Sommerfeld Center, Ludwig-Maximilians-Universität, Theresienstraße 37, D-80333 München, Germany

^dMax-Planck-Institut für Physik (Werner Heisenberg Institut), Föhringer Ring 6, D-80805 München, Germany

E-mail: dgaggero@sissa.it, luca.maccione@lmu.de

Abstract. We model the CR leptonic fluxes above 20 GeV in terms of a superposition of a standard and a charge symmetric extra component, which we generically describe as power-laws in momentum. We investigate under these hypotheses the compatibility between AMS-02, Fermi-LAT and PAMELA datasets on positron fraction, electron+positron spectrum and electron spectrum respectively. We find that it is possible to reconcile AMS and Fermi-LAT data within Fermi-LAT systematics. No compelling evidence of a charge asymmetry in the extra component emerges.

Keywords: cosmic rays; positron fraction; AMS-02

Contents

1	Introduction	1
2	Method	2
3	Results	3
3.1	Analysis of single datasets	3
3.2	Combined analysis	4
4	Conclusions	5

1 Introduction

The AMS collaboration recently published a very accurate measurement of the positron fraction (PF) in cosmic rays (CR) from 0.5 to 350 GeV [1]. The data show the presence of a clear rise above 10 GeV and confirm former experimental results by PAMELA [2] and Fermi-LAT [3]. The AMS collaboration also extended the energy range over which the PF was measured. As a result, the rise of the PF continues up to 250 GeV, while above that energy a precise evaluation of the spectral slope is not possible because of poor statistics. The PF measured by AMS has a lower normalization with respect to Fermi-LAT, and above 50 GeV it is also slightly lower than PAMELA.

Soon after publication of the data, the issue of the mutual compatibility of these datasets was raised in several papers [4, 5]. Analyses were typically performed within phenomenological scenarios in which a “standard” leptonic component originating from acceleration in Supernova Remnants (SNRs) and secondary production in the interstellar medium is added to an extra component with a harder spectrum. The nature of this extra component is still unknown and may be either of astrophysical origin [6–9] or of exotic origin (see [5, 10] and Refs. therein).

Cholis and Hooper [5] showed that, with conventional choices of the standard component and a contribution from DM particles annihilating into leptonic species it is not possible to simultaneously reproduce the AMS PF and Fermi-LAT measurements [11, 12] of the electron+positron (CRE) spectrum. However, models in which DM particles annihilate into light intermediate states which then decay into a combination of muons and charged pions are compatible with those data, provided a hardening in the primary electron excess is assumed. Such hardening may be explained considering the contribution from a local source that accelerates only electrons (e.g. a SNR). On the other hand, Yuan et al. [4] use a Markov Chain MonteCarlo (MCMC) sampler to fit the datasets considering both an astrophysical scenario in which pulsars emit electron+positron pairs and a DM scenario with leptophilic annihilation/decay channels. They also find a tension between AMS PF and Fermi-LAT data, and claim that AMS-02 data require less contribution from the extra component with respect to Fermi-LAT.

These recent results may be understood if a charge asymmetry is present in the extra source [4, 5, 13]. We remark that this might be expected in both exotic and astrophysical scenarios. For example, if DM decays by violating lepton flavor symmetry, it is natural to expect the spectra of the resulting electrons and positrons to be different, both in normalization

and in energy dependence (see e.g. [13] and Refs. therein). If instead the extra source is of astrophysical origin, one possibility is that it includes the contributions of local pulsars and SNRs, not normally accounted for in galactic propagation codes, which would yield charge symmetric and asymmetric contributions, respectively.

Nevertheless, if confirmed the existence of a charge asymmetry would constitute a significant modification of the standard charge symmetric extra-component paradigm studied so far. Luckily enough, the issue is related to high-energy electrons and positrons. If we assume, as in the standard acceleration theory, that CREs are injected in the interstellar medium with a power-law energy spectrum (given that CREs are ultra-relativistic in this energy range, we will always confuse momentum with energy), and if we consider that above a few tens GeV only energy losses and diffusion concur to produce the observed spectrum, then we can approximate the propagated spectra with power-laws without losing generality. We can therefore apply standard data analysis techniques to study the properties of the observed spectra in a model independent way.

This is the purpose of the present paper, that is composed as follows. In Section 2 we will discuss our methodology, including the assumptions we make and the numerical tools we use in our study. In Section 3 we will show the results of our investigation. Finally, in Section 4 we will draw our conclusions.

2 Method

We want to analyze the compatibility of the following 3 data sets in the high energy range: a) Fermi-LAT [11, 12] and HESS [14] spectra of $e^+ + e^-$; b) PAMELA spectrum of e^- only [3]; c) AMS positron ratio $e^+/(e^+ + e^-)$ [1]. Above 20 GeV the effects of solar modulation, re-acceleration and convection are negligible. Moreover, the contribution of secondary electrons and positrons is negligible at these energies. Therefore, the propagated spectrum can only be affected by [15]:

- The energy dependent escape from the galaxy, described by the diffusion coefficient, typically assumed as $D = D_0(\rho/\rho_0)^\delta$, where ρ is the particle rigidity and δ is a constant parameter;
- Continuous energy losses, including ionization, coulomb scattering and bremsstrahlung in the interstellar gas, synchrotron losses in the galactic magnetic fields and inverse Compton scattering off interstellar radiation fields. However, above 100 GeV synchrotron and inverse Compton losses are the dominant processes, as we show in Fig. 1 for the gas, magnetic and radiation field models typically used in Galprop [16, 17] and DRAGON [18–20]. At 20 GeV the maximal contribution of the other processes is $\sim 25\%$ and it decreases with increasing energy, becoming of the order of a few % at 100 GeV. We remark that for both synchrotron and inverse Compton processes $dE/dt \propto E^2$ in the ultra-relativistic Thomson regime.

In these conditions, it is well known [21] that if a power-law energy (or momentum) spectrum is injected by CRE sources, then a power-law spectrum, with a possibly different slope and with breaks, is to be expected after propagation. In fact, we checked that in the energy range we are considering a pure power-law is expected after propagation. We can then assume with confidence, for our purposes, that the propagated spectra be perfect power-laws, plus some exponential cutoff at high energy, describing a possible cutoff at injection or the

cutoff induced by the energy loss length becoming shorter than the typical distance between the Earth and the closest CRE sources. We start our analysis by assuming the presence of 2 components:

Component A a primary electron component with spectrum $J_A = A \times (E/E_0)^{-\alpha} \exp(-E/E_{\text{cut},A})$

Component B an extra component of electrons and positron with spectrum $J_B = B \times (E/E_0)^{-\beta} \exp(-E/E_{\text{cut},B})$,

where $E_0 = 20$ GeV and the units of the parameters will be $\text{GeV}^{-1}\text{m}^{-2}\text{sr}^{-1}\text{s}^{-1}$ for A and B , TeV for $E_{\text{cut},B}$, while α and β are numbers. In this model-independent parametrization: a) the Fermi-LAT and HESS spectra are described by $J_A + 2 \cdot J_B$, b) the PAMELA electron spectrum is $J_A + J_B$, and c) the AMS PF is $J_B/(J_A + 2 \cdot J_B)$.

Given that it is irrelevant in the analysis, because the primary electron components falls off very steeply with increasing energy, we fix the value of $E_{\text{cut},A} = 10$ TeV. With this choice, we are left with 5 free parameters. We use therefore a Markov Chain MonteCarlo (MCMC) algorithm to estimate the probability density functions of the parameters. We exploit the Bayesian Analysis Toolkit (BAT) [22, 23] to perform the MonteCarlo scan and the analysis.

This setup is valid in the case of a charge symmetric extra-component. In order to study also charge asymmetric scenarios, we will introduce two possibilities. First, we will consider the case in which the electron and positron spectra of the extra component differ only in normalization. We will then introduce a parameter ϵ such that electrons correspond to $(1 + \epsilon)J_B$ and positrons to $(1 - \epsilon)J_B$. On the other hand, we will also consider the presence of a pure electron component C , such that $J_C = C(E/E_0)^{-\gamma} \exp(-E/E_{\text{cut},C})$, such that the electron and positron spectra of the total extra-component (B+C) may differ also in slope.

As a final remark, we note that with our formalism we cannot capture any irregular behavior of the extra component, as expected if several individual local sources contribute to it [24]. However, neither Fermi-LAT nor AMS-02 data show hints of this behavior, therefore we will neglect this possibility in the following.

3 Results

We first consider our datasets separately, then we perform a combined analysis. In Figs. 2 ÷ 6 we summarize the main results. The plots show the probability density function sampled with the BAT for one and two-dimensional slices of the full parameter space.

3.1 Analysis of single datasets

We show in Figures 2, 3 and 4 the results of the analysis of the individual datasets of AMS-02, PAMELA and Fermi-LAT respectively. The AMS analysis (Fig. 2) shows a high degeneracy between most parameters, and does not point towards a well defined region in the parameter space. Of particular interest are the correlation plots for A - B and α - β . The two couples of parameters are very tightly correlated, indicating that a high degeneracy exists between the two components A and B . This is not unexpected for the positron ratio data. Indeed, no matter how steep the primary component A is taken, it is always possible to find a corresponding index for the component B that produces a good fit for the ratio. Moreover, the posterior probability distribution for most of the parameters is flat, indicating that the positron fraction alone cannot disentangle the contributions of the two components.

A similar situation would hold for the PAMELA only analysis (Fig. 3) if we would only account for the positron fraction data. Since instead we include in this analysis only the electron spectrum measured by PAMELA, which is described very well by a single power-law, the degeneracy α - β is broken. In order to explain PAMELA electron data we do not need an extra component, and simply fitting the parameters of component A would be enough.

The Fermi-LAT analysis, instead, isolates a particular region in the parameter space (Fig. 4). By looking at the α - β correlation plot we can notice that a very narrow range of values for the two injection indexes is able to produce the observed slope of the electron+positron spectrum. However, while the preferred value of α is very well compatible, within uncertainties, with the value preferred by PAMELA, Fermi-LAT data point to very small values of β , which are about 2σ away from the values preferred by PAMELA and also by AMS-02. This fact might already hint at the presence of some mild tension between the datasets. We also notice that Fermi-LAT data are able to constrain the cutoff energy of the B component rather strongly, to $E_{\text{cut},B} \simeq 1.3$ TeV.

3.2 Combined analysis

Let us turn now our attention to the combined AMS and PAMELA analysis. From Fig. 5 it is clear that the confidence regions for the two experiments nicely overlap. Moreover, by combining the electron spectrum of PAMELA with the high accuracy data of AMS-02 we can better pin-point the slope β of the B component.

Concerning the combined AMS-02 and Fermi-LAT analysis, the situation is more complicated. Comparing Fig. 2 and Fig. 4 it is clear that the maximum likelihood regions of AMS and Fermi-LAT do not show any overlap. The best-fit regions for AMS-02 correspond to a poor fit of Fermi-LAT data and vice-versa. The combined analysis (Fig. 6) selects an intermediate region of the parameter space different from the individual regions preferred by Fermi-LAT and AMS-02, and the best-fit corresponds to the plot shown in Figures 7 and 8. It is very important to point out now that only the statistical errors were taken into account in this analysis. If we further account for systematic errors in Fermi-LAT measurements, the combined best-fit is not in strong tension with Fermi-LAT dataset, as clearly seen in Fig. 8. The reduced χ^2 for the combined fit in this case (adding systematic and statistical errors in quadrature) is 0.75.

On the other hand, if we instead allow for an asymmetry in component B , with electrons corresponding to $(1 + \epsilon)J_B$ and positrons to $(1 - \epsilon)J_B$, we find a clear indication for $\epsilon \simeq 0.22$, while the spectral parameters of the component B are not strongly affected (the parameters of the “background” component A vary more strongly because of the additional electron contribution from the asymmetric B component). Also in the scenario with component C we find an indication of a possible presence of a very hard component ($\gamma \simeq 2$) active at relatively low energies, with $E_{\text{cut},C} \simeq 300$ GeV. Its normalization is however at the level of 10^{-3} , about 5 orders of magnitude smaller than the other components, hinting at the fact that it might be only a mathematical artefact of the fitting procedure. In both cases however the improvement on the global fit is modest (reduced χ^2 improving from 0.75 to 0.64), even though the improvement on the AMS-02 PF is intriguing, with a reduced χ^2 passing from 1.36 without asymmetry to 1.18 for the best-fit model shown in the second row of Tab. 1. An F -test [25] however, shows that this improvement is not sufficient to claim evidence for charge asymmetry at the 95% confidence level. We show in Figures 7 and 8 a comparison between our best-fit models with and without charge asymmetry for the PF and the CRE spectra respectively. The charge asymmetric model slightly improves the agreement with

Table 1. Best fit values and 1σ uncertainties for the parameters of our charge symmetric and charge asymmetric models. The model including component C is not shown.

A	α	B	β	$E_{\text{cut,B}}$	ϵ
140 ± 1	3.166 ± 0.003	9.08 ± 0.09	2.61 ± 0.01	1.6 ± 0.1	0 (fixed)
135 ± 1	3.193 ± 0.004	11.76 ± 0.22	2.63 ± 0.01	1.6 ± 0.1	0.22 ± 0.02

the AMS-02 PF data at the highest energy points, but has only a very small impact on the agreement with Fermi-LAT data.

4 Conclusions

We considered a model independent parametrization of the CR leptonic spectra as the superposition of a standard component plus an extra charge-symmetric component. The spectra are modeled as power-laws in energy. We exploited Fermi-LAT, PAMELA and AMS-02 datasets and analyzed their mutual compatibility within this framework with a MCMC algorithm and using Bayesian inference. We report in Tab. 1 the best fit values of our parameters with their uncertainties. The confidence regions in the parameter space for Fermi-LAT and AMS do not overlap, but the combined analysis produces a best-fit model which is good for AMS, and not in strong tension with Fermi-LAT, especially if we take into account the presence of systematic uncertainties. We also considered charge asymmetric scenarios for the extra-component and showed that they do not lead to substantial improvements to the fits. Therefore, the two datasets of AMS-02 and Fermi-LAT are compatible within systematic errors and no compelling need for a charge asymmetry of the extra component emerges.

Acknowledgments

We warmly thank Dario Grasso, Carmelo Evoli and Piero Ullio for reading the draft of this paper and providing useful insights. DG thanks Piero Ullio and Wei Xue for inspiring discussions and the Max-Planck-Institute for Physics for warm hospitality during the initial phase of this work. LM acknowledges support from the Alexander von Humboldt foundation and partial support from the European Union FP7 ITN INVISIBLES (Marie Curie Actions, PITN- GA-2011- 289442).

References

- [1] **AMS Collaboration** Collaboration, M. Aguilar et al., *First Result from the Alpha Magnetic Spectrometer on the International Space Station: Precision Measurement of the Positron Fraction in Primary Cosmic Rays of 0.5350 GeV*, *Phys.Rev.Lett.* **110** (2013), no. 14 141102.
- [2] **PAMELA Collaboration** Collaboration, O. Adriani et al., *An anomalous positron abundance in cosmic rays with energies 1.5-100 GeV*, *Nature* **458** (2009) 607–609, [[arXiv:0810.4995](#)].
- [3] **PAMELA Collaboration** Collaboration, O. Adriani et al., *The cosmic-ray electron flux measured by the PAMELA experiment between 1 and 625 GeV*, *Phys.Rev.Lett.* **106** (2011) 201101, [[arXiv:1103.2880](#)].
- [4] Q. Yuan and X.-J. Bi, *Reconcile the AMS-02 positron fraction and Fermi-LAT/HESS total e^\pm spectra by the primary electron spectrum hardening*, [arXiv:1304.2687](#).

- [5] I. Cholis and D. Hooper, *Dark Matter and Pulsar Origins of the Rising Cosmic Ray Positron Fraction in Light of New Data From AMS*, [arXiv:1304.1840](#).
- [6] D. Hooper, P. Blasi, and P. D. Serpico, *Pulsars as the Sources of High Energy Cosmic Ray Positrons*, *JCAP* **0901** (2009) 025, [[arXiv:0810.1527](#)].
- [7] P. Blasi, *The origin of the positron excess in cosmic rays*, *Phys.Rev.Lett.* **103** (2009) 051104, [[arXiv:0903.2794](#)].
- [8] P. Mertsch and S. Sarkar, *Testing astrophysical models for the PAMELA positron excess with cosmic ray nuclei*, *Phys.Rev.Lett.* **103** (2009) 081104, [[arXiv:0905.3152](#)].
- [9] M. Ahlers, P. Mertsch, and S. Sarkar, *On cosmic ray acceleration in supernova remnants and the FERMI/PAMELA data*, *Phys.Rev.* **D80** (2009) 123017, [[arXiv:0909.4060](#)].
- [10] T. Linden and S. Profumo, *Probing the Pulsar Origin of the Anomalous Positron Fraction with AMS-02 and Atmospheric Cherenkov Telescopes*, [arXiv:1304.1791](#).
- [11] **Fermi LAT Collaboration** Collaboration, A. A. Abdo et al., *Measurement of the Cosmic Ray e^+ plus e^- spectrum from 20 GeV to 1 TeV with the Fermi Large Area Telescope*, *Phys.Rev.Lett.* **102** (2009) 181101, [[arXiv:0905.0025](#)].
- [12] **Fermi LAT Collaboration** Collaboration, M. Ackermann et al., *Fermi LAT observations of cosmic-ray electrons from 7 GeV to 1 TeV*, *Phys.Rev.* **D82** (2010) 092004, [[arXiv:1008.3999](#)].
- [13] I. Masina and F. Sannino, *Hints of a Charge Asymmetry in the Electron and Positron Cosmic-Ray Excesses*, [arXiv:1304.2800](#).
- [14] **H.E.S.S. Collaboration** Collaboration, F. Aharonian et al., *Probing the ATIC peak in the cosmic-ray electron spectrum with H.E.S.S.*, *Astron.Astrophys.* **508** (2009) 561, [[arXiv:0905.0105](#)].
- [15] V. S. Berezinskii, S. V. Bulanov, V. A. Dogiel, and V. S. Ptuskin, *Astrophysics of cosmic rays*. 1990.
- [16] “The galprop code for cosmic-ray transport and diffuse emission production.” <http://galprop.stanford.edu/>.
- [17] A. W. Strong, I. V. Moskalenko, and V. S. Ptuskin, *Cosmic-ray propagation and interactions in the Galaxy*, *Ann.Rev.Nucl.Part.Sci.* **57** (2007) 285–327, [[astro-ph/0701517](#)].
- [18] “Dragon code.” <http://dragon.hepforge.org/>.
- [19] G. Di Bernardo, C. Evoli, D. Gaggero, D. Grasso, and L. Maccione, *Unified interpretation of cosmic-ray nuclei and antiproton recent measurements*, *Astropart.Phys.* **34** (2010) 274–283, [[arXiv:0909.4548](#)].
- [20] G. Di Bernardo, C. Evoli, D. Gaggero, D. Grasso, L. Maccione, et al., *Implications of the Cosmic Ray Electron Spectrum and Anisotropy measured with Fermi-LAT*, *Astropart.Phys.* **34** (2011) 528–538, [[arXiv:1010.0174](#)].
- [21] S. V. Bulanov and V. A. Dogel, *The Influence of the Energy Dependence of the Diffusion Coefficient on the Spectrum of the Electron Component of Cosmic Rays and the Radio Background Radiation of the Galaxy*, *Astrophys. J. Suppl. Series* **29** (Aug., 1974) 305–318.
- [22] “Bat – bayesian analysis toolkit.” <http://www.mppmu.mpg.de/bat/>.
- [23] A. Caldwell, D. Kollár, and K. Kröninger, *BAT - The Bayesian analysis toolkit*, *Computer Physics Communications* **180** (Nov., 2009) 2197–2209, [[arXiv:0808.2552](#)].
- [24] D. Malyshev, I. Cholis, and J. Gelfand, *Pulsars versus Dark Matter Interpretation of ATIC/PAMELA*, *Phys.Rev.* **D80** (2009) 063005, [[arXiv:0903.1310](#)].
- [25] P. R. Bevington and D. K. Robinson, *Data reduction and error analysis for the physical sciences*. 1992.

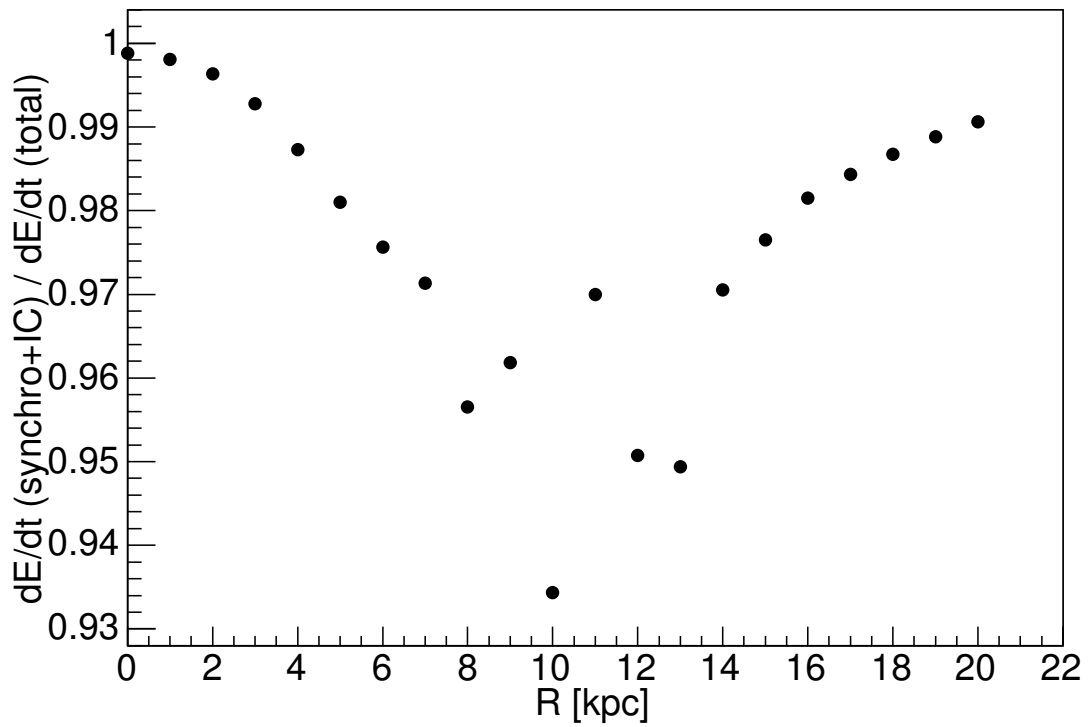


Figure 1. Radial dependence of the ratio of energy loss rates for synchrotron and inverse Compton process with respect to the total energy loss rate on the galactic plane for ~ 100 GeV electrons.

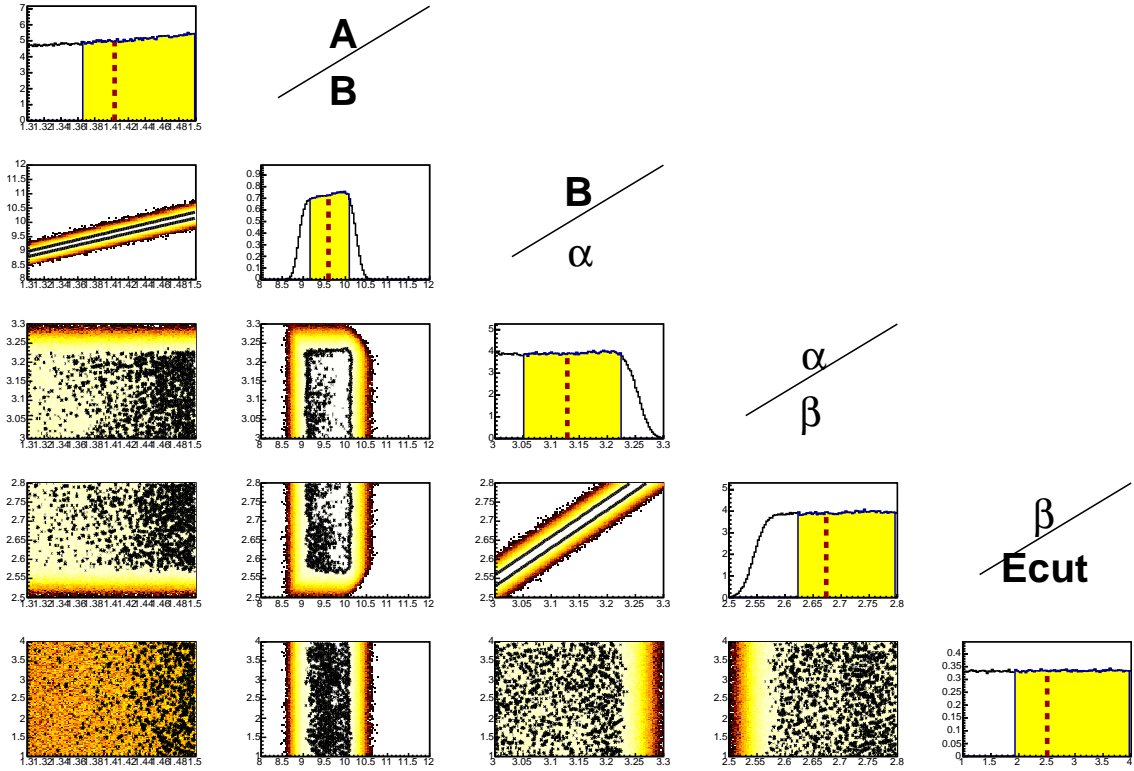


Figure 2. Posterior probability distribution and correlation plots for the model parameters using AMS-02 data. The upper (lower) labels indicate the content present in the row (column). The plots should be read in matrix form. A ii -type plot (the ones on the diagonal) represents the posterior probability distribution of a single parameter, with the yellow region highlighting the 68% confidence area and the vertical red dashed line the median value. A ij -type plot shows instead the correlation between parameters i and j . To improve readability we show the values of the parameter A (fits column) divided by 100.

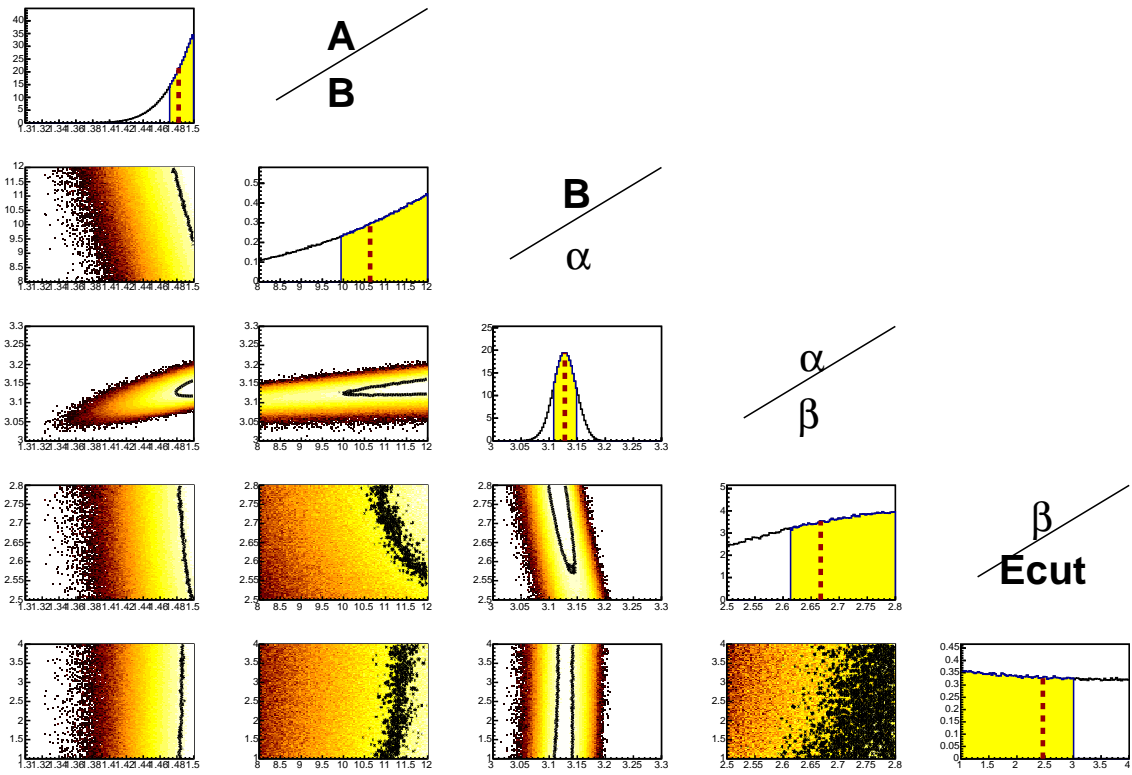


Figure 3. Same as 2 for Pamela data.

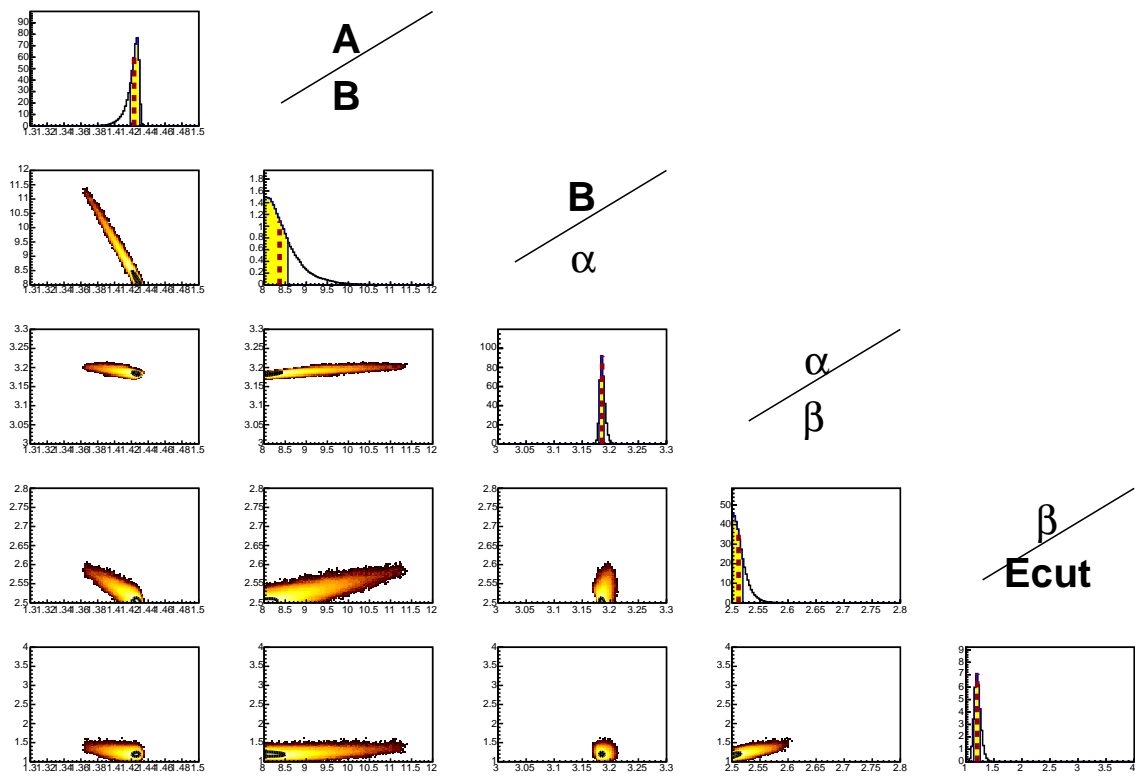


Figure 4. Same as 2 for Fermi-LAT data.

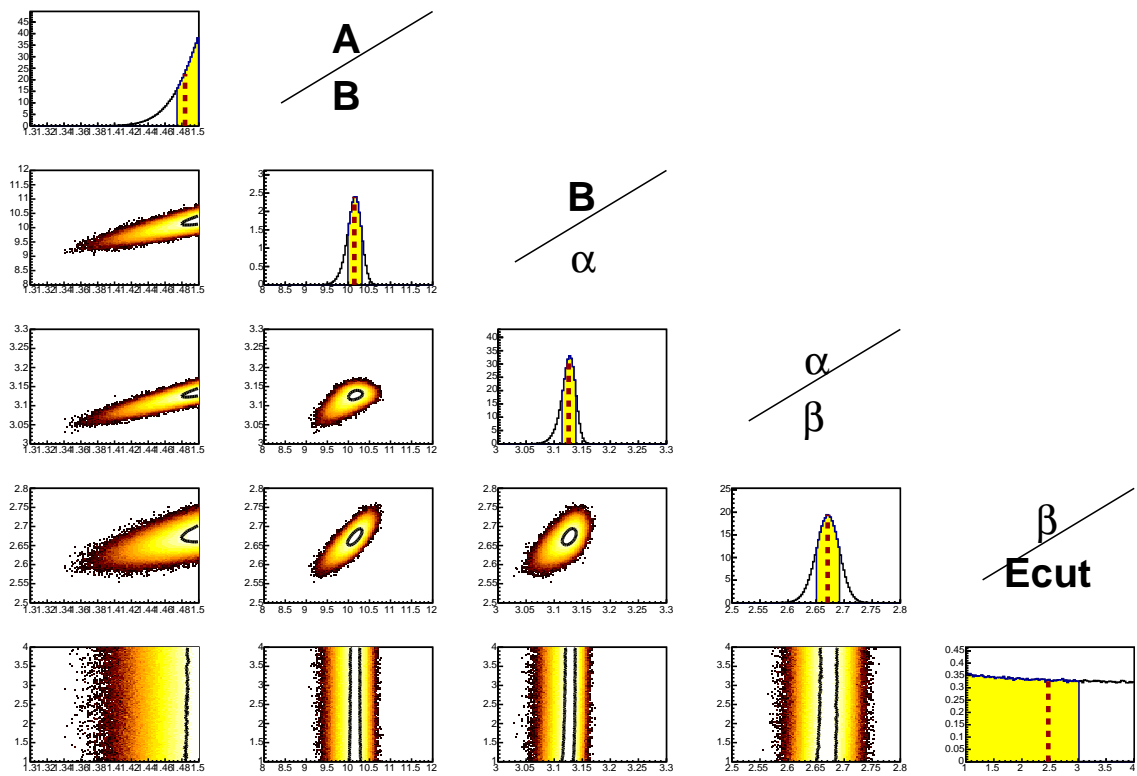


Figure 5. Same as 2 for the combined AMS-02 and PAMELA data.

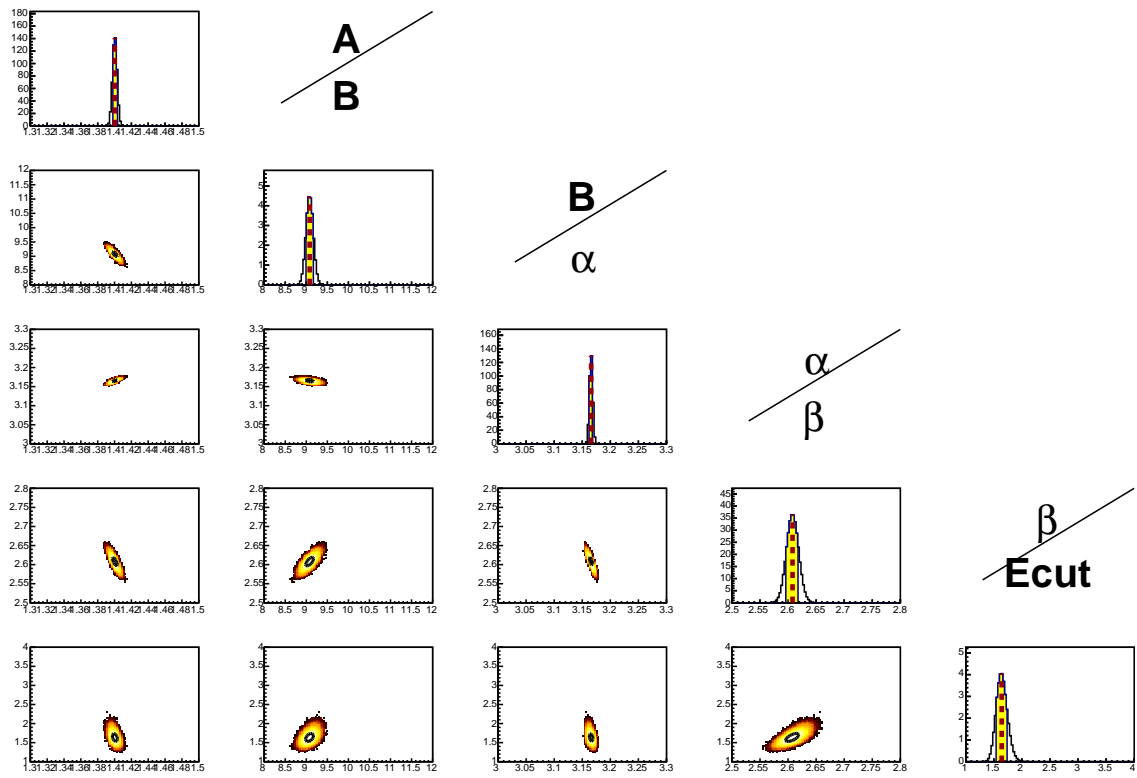


Figure 6. Same as 2 for the combined AMS-02 and Fermi-LAT data.

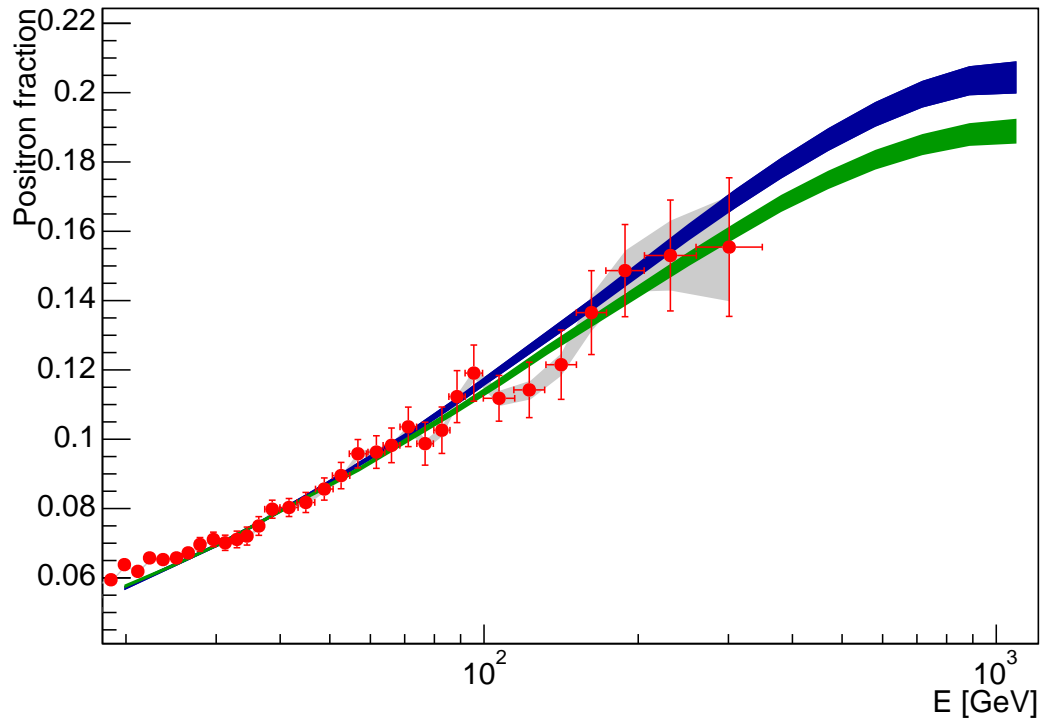


Figure 7. Positron fraction for the best fit model derived combining AMS-02 and Fermi-LAT data. Red points are AMS-02 experimental data. The blue area represents our best-fit model, with its 68% uncertainty band. The green area is instead for the best fit model assuming charge asymmetry. Error bars are statistical errors, while systematic errors correspond to the grey band.

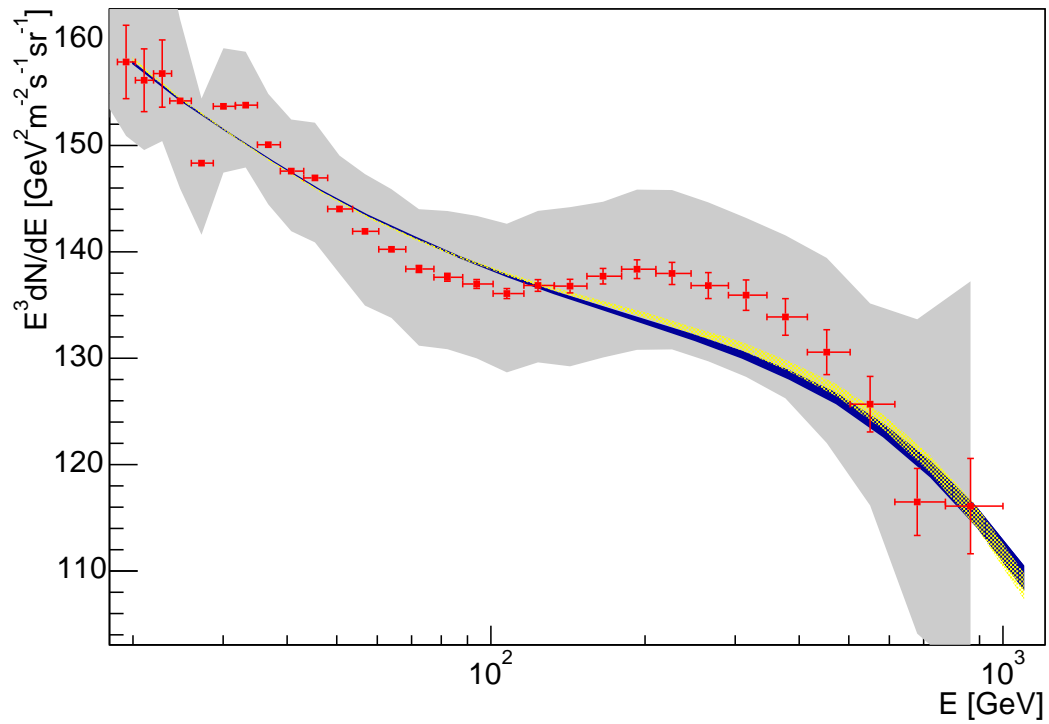


Figure 8. CRE spectrum for the best fit model derived combining AMS-02 and Fermi-LAT data. Red points are Fermi-LAT experimental data. The blue area represents our best-fit model, with its 68% uncertainty band. The yellow dotted area is instead for the best fit model assuming charge asymmetry. Error bars are statistical errors, while systematic errors correspond to the grey band.